Supporting Information

Accelerating Bone Regeneration in Cranial Defects Using an Injectable Organic-Inorganic Composite Hydrogel

Qiao Bian,[a] Chao Guo,[c] Shuquan Cui,[b] Jia Liu,[c] Guohua Xu*[c] and Wei Feng*[a]

[a] *Department of Chemistry, State Key Laboratory of Molecular Engineering of Polymers, Collaborative Innovation Center of Chemistry for Energy Materials, Fudan University, Shanghai 200438, China. Email: fengweifd@fudan.edu.cn*

[b] *State Key Laboratory of Molecular Engineering of Polymers, Department of Macromolecular Science, Fudan University, Shanghai 200438, China*

[c] *Department of Orthopedic Surgery, Spine Center, Changzheng Hospital, Second Military Medical University of the Chinese People's Liberation Army, Shanghai 200003, China. Email: xuguohuamail@smmu.edu.cn*

2. Materials and methods

2.2. Composite preparation

2.2.1. Synthesis of PCLA-PEG-PCLA triblock copolymers. Briefly, PEG 1500 (15 g, 10 mmol) was added into a 250-mL three-neck flask and dried under vacuum at 120 °C for 2 h. After the system was cooled to 60 °C, LA (25.79 g, 179 mmol), CL (10.21 g, 89.5 mmol), and $Sn(Oct)_2$ (0.4 wt% of the total mass of monomers) were added, followed by vacuum treatment for 30 min. Then, the polymerization reaction lasted with mechanical stirring at 150 °C under an argon atmosphere for 12 h. The product was washed with water of 80 °C three times and freeze-dried.

2.3. Characterization of SIM/ (Sr/β-TCP)/PCLA-PEG-PCLA composite

2.3.2. Scanning electron microscope (SEM) of β-TCP and $SrHPO_4$. For SEM, a trace amount of inorganic powder was dispersed in ethanol by ultrasound for 30 min, and then a drop of solution was added to the copper conductive adhesive. The ethanol was gradually volatilized at room temperature, and the excess powder samples were blown away with a high-pressure dust removal gas tank. The sample was gilded with a high-vacuum ion sputtering instrument and then imaged by SEM with an accelerating voltage of 8 kV. For XRD experiment, 1 g β-TCP or hydroxyapatite (HAP) was immersed in 10 mL SBF in the shaking bath for 7 days. The supernatant was replaced by fresh SBF every 2 days. On the 7th day, the powder of inorganic substances was dried for the XRD test. The scan range was 10-80° and the scanning rate was 10°/min.

2.3.3. Transmission electronic microscope (TEM) and dynamic light scattering (DLS) of blending solutions. For TEM, a small amount of polymer (1 wt%) without or with SIM (0.16 mg/g) solution was dropped on a copper grid and dried at room temperature overnight. The acceleration voltage was 200 kV. For DLS measurements, the measurement was carried out with a scattering angle of 90°. The polymer concentration was 1 wt% and the SIM concentration was 0.16 mg/g. Before the measurement, the sample was filtered through a 0.45 μm filter to remove possible dust. The measurement was conducted after a 10-min equilibration at 25 °C.

2.3.4. Rheological characterization of blending systems. The test temperature

was set from 15 °C to 45 °C with a heating rate of 1 °C /min. In brief, approximately 1.5 mL solution was transferred to the basal plate, whose margin was overlaid with a thin layer of low-viscosity silicone oil to minimize water evaporation. The gap between the basal plate and the cone plate was set to 0.052 mm with an angular frequency of 10 rad/s and stress of 5 Pa.

2.4. In vitro release of SIM

In each glass bottle, 0.5 g solution was added to its bottom, and then the glass bottle was placed in the shaking bath at 37 °C. After the spontaneous gelation, 50 mL synthermal PBS (with 0.5 wt% tween 80 and 0.025 wt% NaN_3) was gently added.

The in vitro release of SIM was recorded at predetermined time points (day 0,7,14, 28, 42, 56, and 63). Because of the instability of SIM in PBS, the drug content was detected in the residual gel, rather than the supernatant. Briefly, we first removed the supernatant, then dissolved the residual gel with ultrapure water and freeze-dried the blends. After that, a certain amount of acetonitrile was added to extract SIM. The extraction was diluted before the measurement. The release amount was calculated based on the standard curve.

2.5. Cell toxicity assay

2.5.2. In vitro cytotoxicity assay of polymers. MC3T3-E1 cells (5000 /well) were seeded in 96-well plates and cultured for 12 h. Then the culture medium was replaced with 200 μL fresh medium containing different concentrations of polymer. The actual concentrations of polymer were 0.001, 0.005, 0.01, 0.05, 0.1 0.5, 1, and 2 wt%. After 24 h and 48 h of incubation respectively, the old medium was replaced by the fresh medium with 10% CCK-8 solution for another incubation of 2-2.5 h.

2.5.3 In vitro cytotoxicity assay of hydrogels. In brief, the extracts were removed and cells were incubated with a mixture of propidium iodide and calcein AM in phosphate buffered saline (PBS) at 37 °C for 30 min. Then, the staining solution was replaced by PBS, followed by the microscopic observations of the fluorescent staining via an inverted fluorescence microscope (Zeiss, Axio Observer 7).

2.6. Cell differentiation assay

2.6.2. Cell differentiation assay. For osteogenic induction, the composition of osteogenic induction medium was as follows: 90% high-glucose DMEM (Gibco, Thermofisher), 10% FBS, 100 U/mL penicillin, 100 μg/mL streptomycin, 100 nM dexamethasone, 50 μM trisodium ascorbate 2-phosphate, and 10 mM sodium β-glycerophosphate. On the 3rd day, we began to add 5 μg/mL aphidicolin additionally to inhibit cell proliferation and replaced the medium every 2 days. The osteogenic differentiation was conducted qualitatively and quantitatively on the 7th and 14th day.

2.6.3. BCIP/NBT alkaline phosphatase and alizarin Red S Staining. The cells were treated by following the operation manual. In brief, the cells were fixed with a 4% paraformaldehyde solution (Servicebio, Wuhan) for 15 min, and were stained with a staining working solution for 30 min. After that, the solution was removed and further rinsed with PBS. Images were captured with an inverted fluorescence microscope.

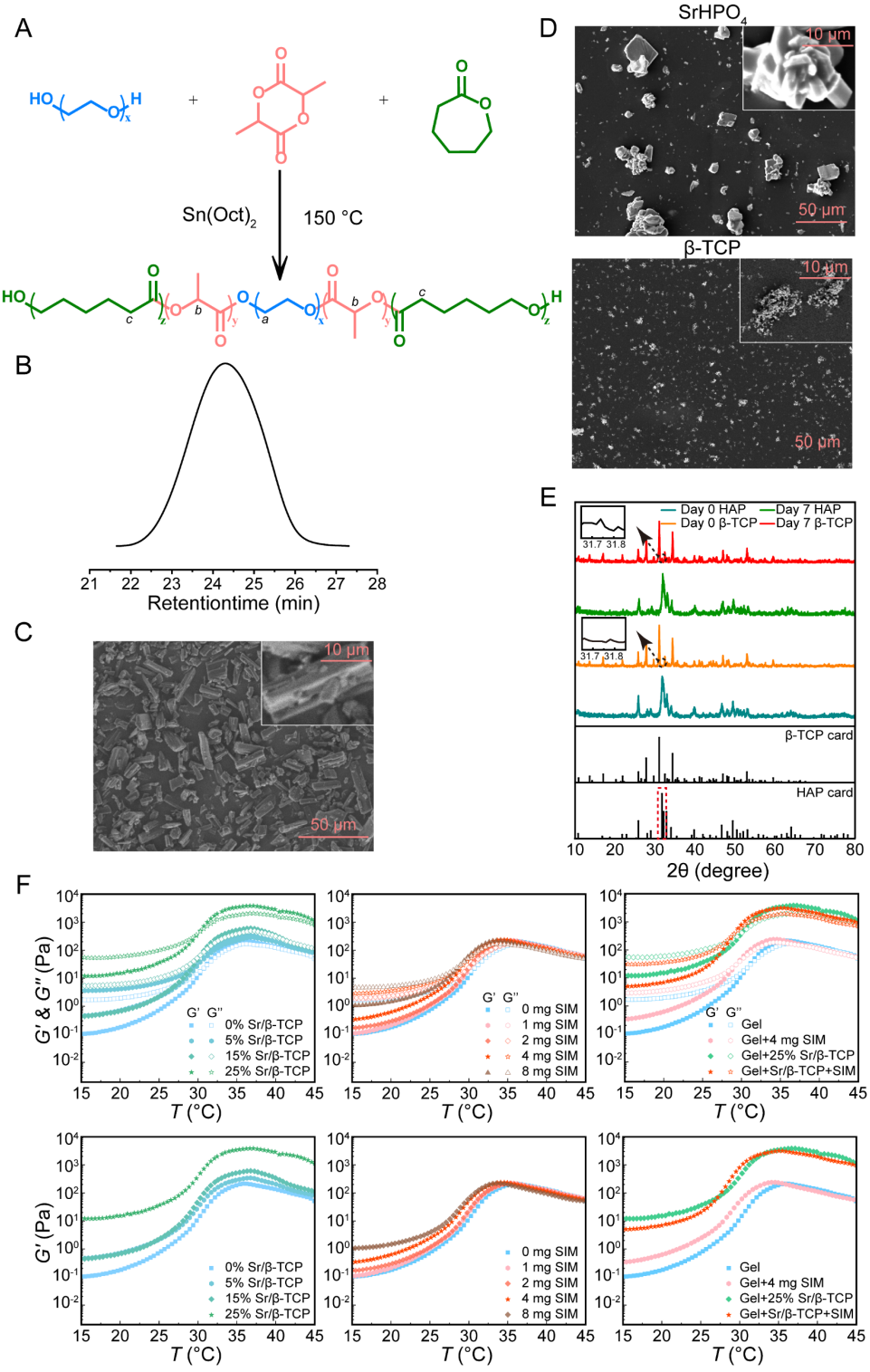

Fig. S1 Supplementary characterization of materials. (A) The schematic synthesis route of triblock copolymer. (B) GPC trace of PCLA-PEG-PCLA. (C) The SEM images of SIM. (D) SEM images of $SrHPO_4$ and β-TCP. (E) The XRD spectrum changes of inorganics in SBF for 7 days. (F) Rheological behaviors of the indicated aqueous systems upon heating.

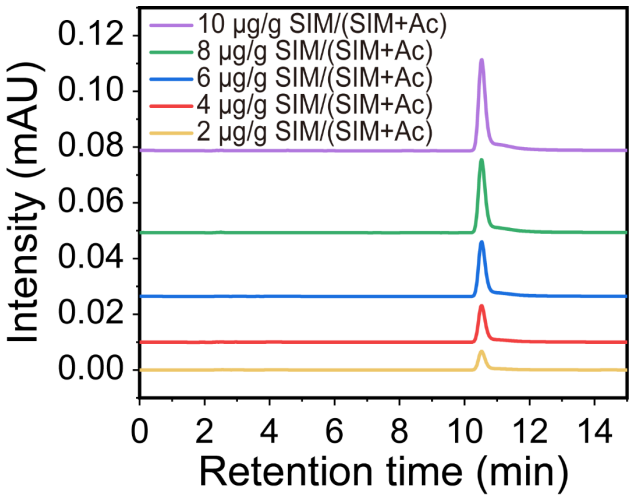

Fig. S2 The HPLC traces of SIM in acetonitrile.

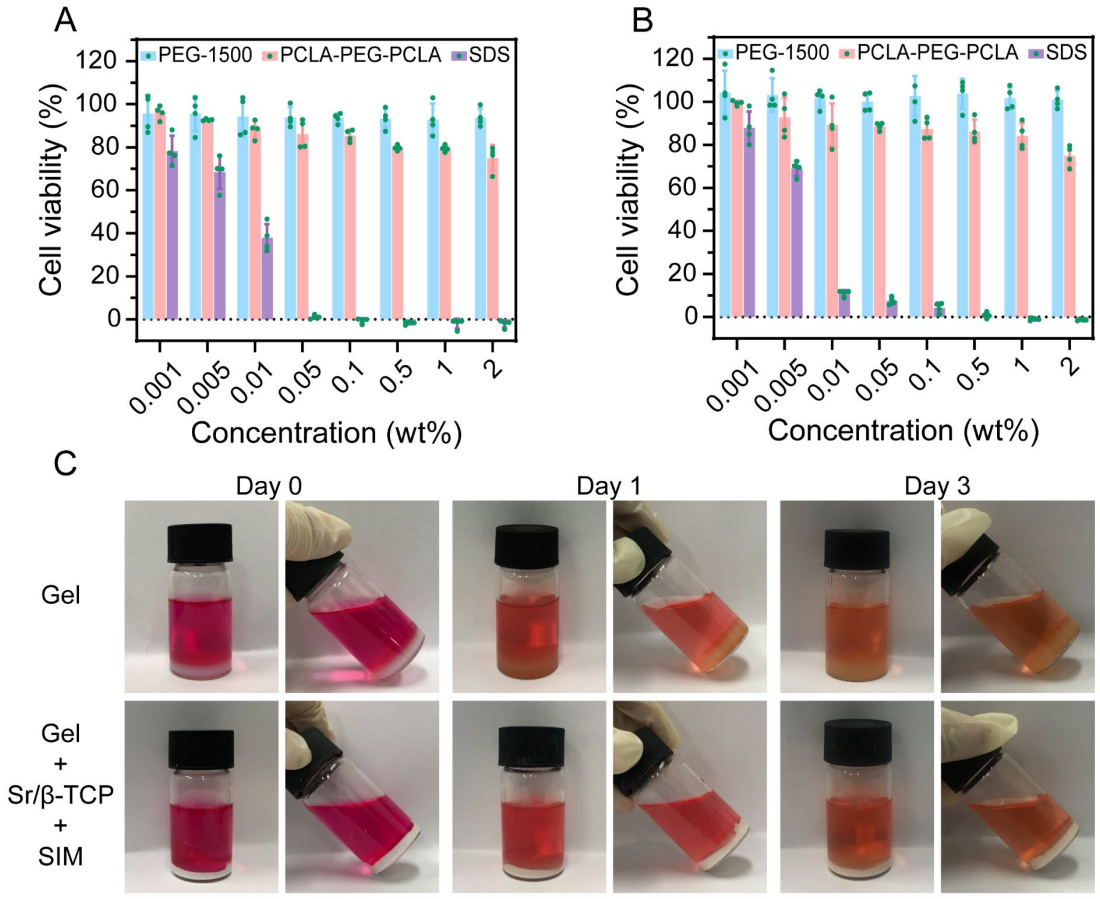

Fig. S3 The cell cytotoxicity of triblock copolymer and blending hydrogels. Cell viability of PCLA-PEG-PCLA solution with gradient concentration for (A) 24 h and (B) 48 h. (C) The diagrammatic sketch of extraction process of blending hydrogels.

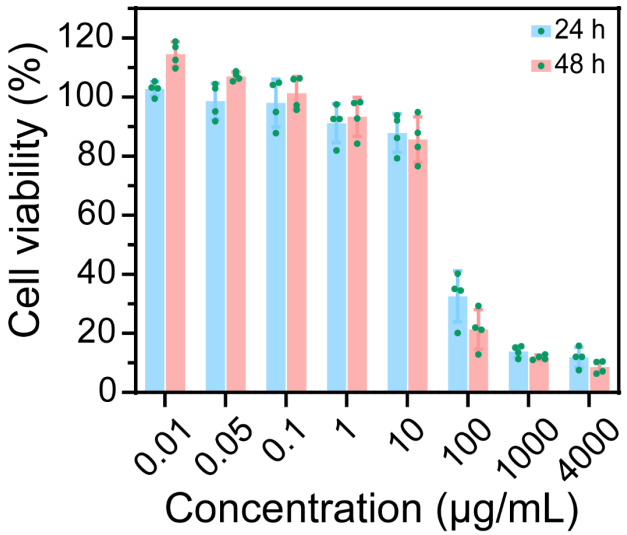

Fig. S4 The cell cytotoxicity of drug. Cell viability of SIM solution with gradient concentration for 24 h and 48 h.

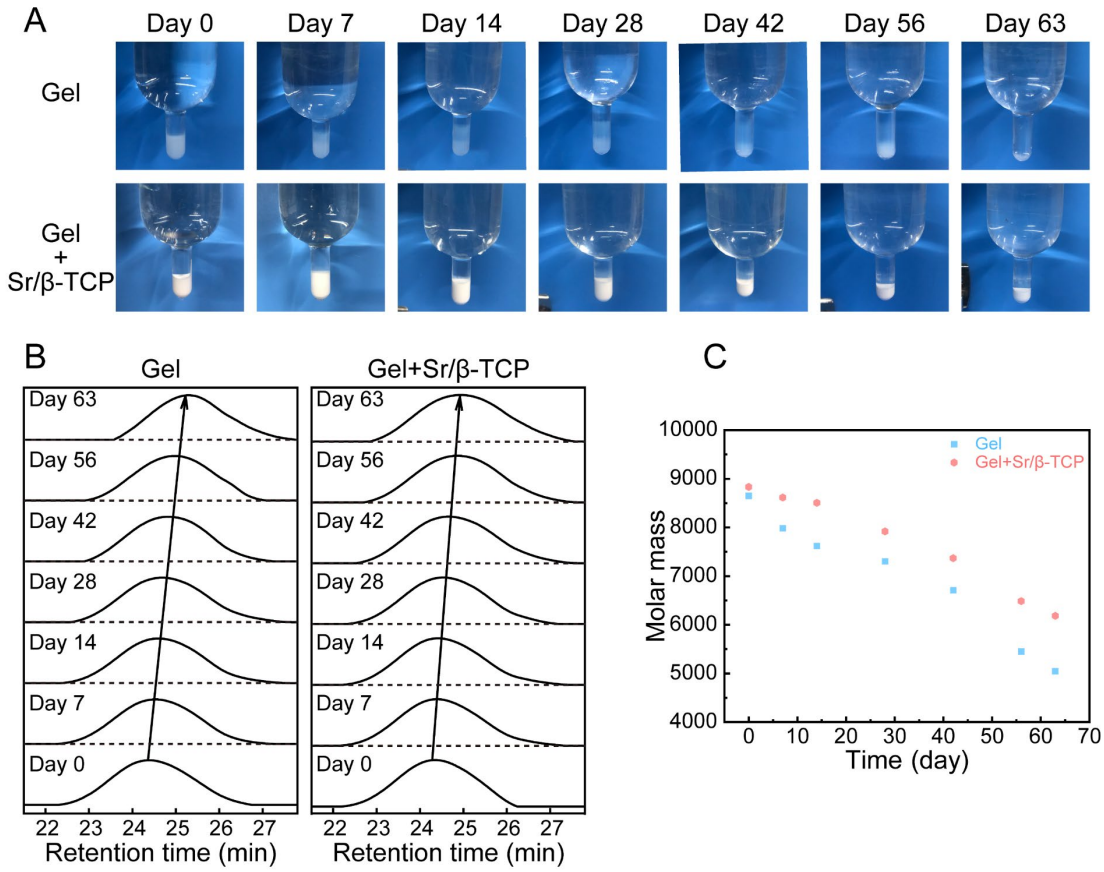

Fig. S5 In vitro degradation of the indicated groups. (A) The representative optical photographs of remaining hydrogels in vitro (n=3). (B) GPC traces and (C) M_{peak} of remaining hydrogels at the predetermined time points.

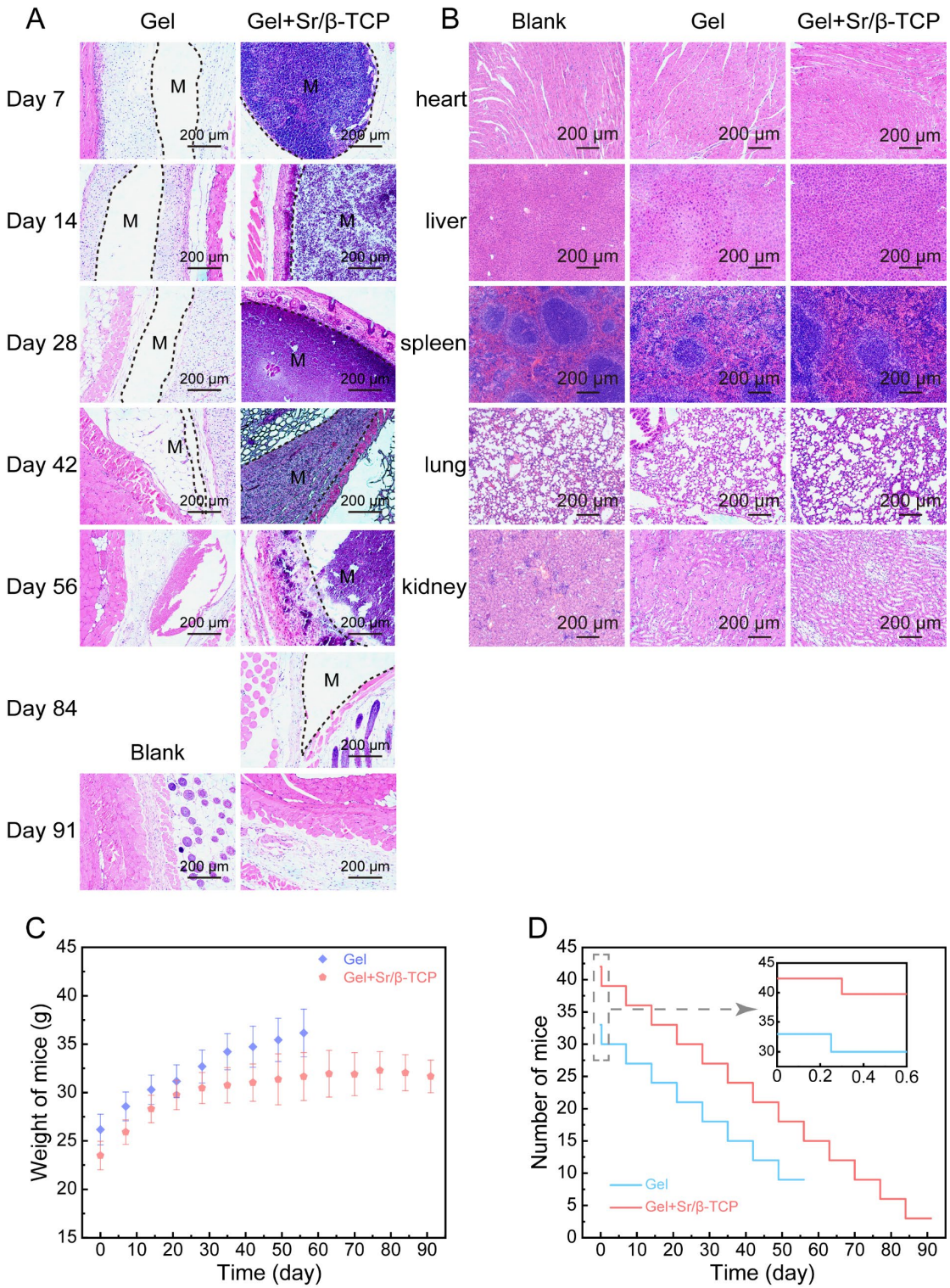

Fig. S6 Biocompatibility of the indicated groups in mice. (A) H&E staining images of surroundings of remaining hydrogel in mice ("M" denotes material). (B) Histological analysis of major organs of mice in the indicated groups. (C)The weight and (D) number of surviving mice of the indicated groups at predetermined days.

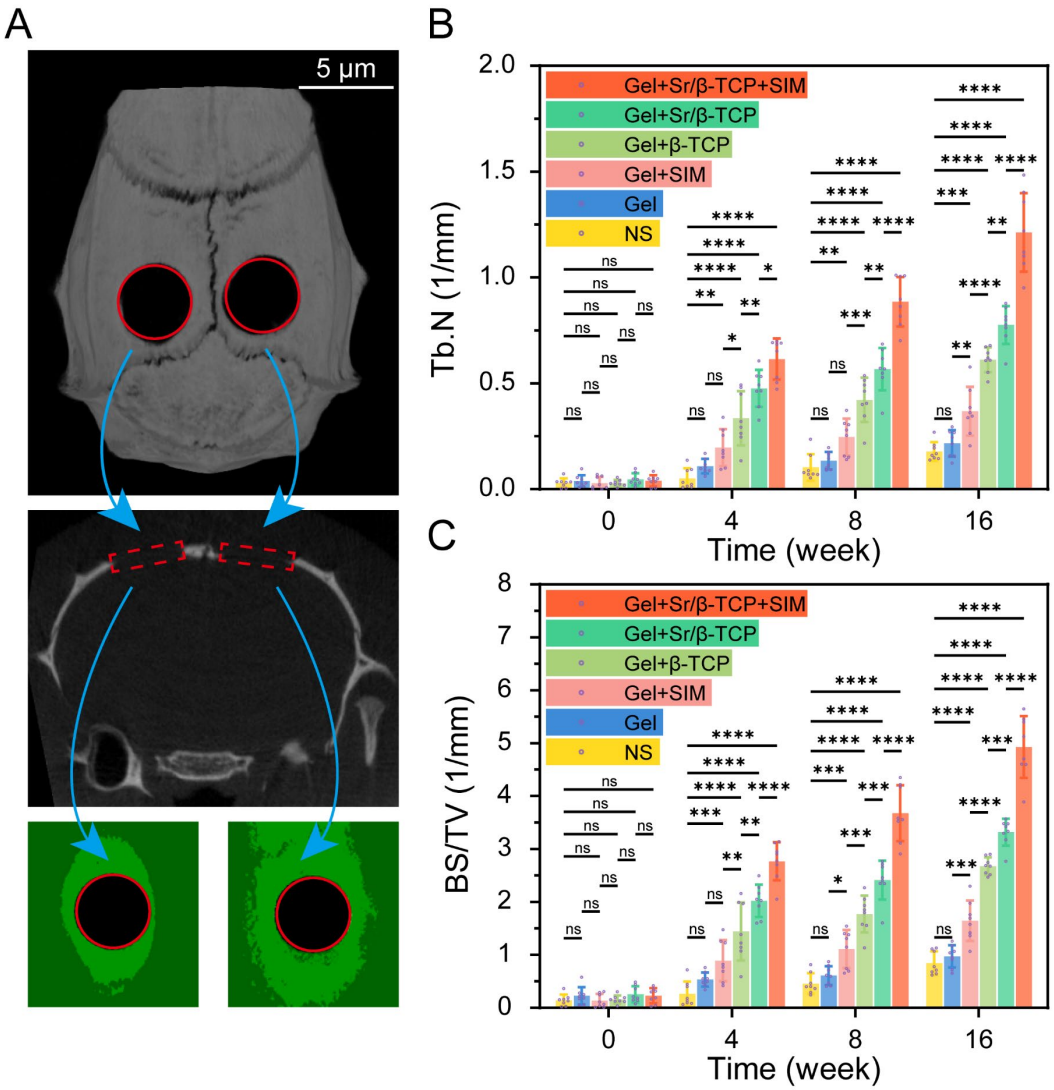

Fig. S7 (A) The Simple schematic diagram of processing and calculation of micro-CT data. (B) Trabecular number and (C) bone surface density of the indicated groups on the day of surgery and in the 4th, 8th, and 16th week postsurgery.

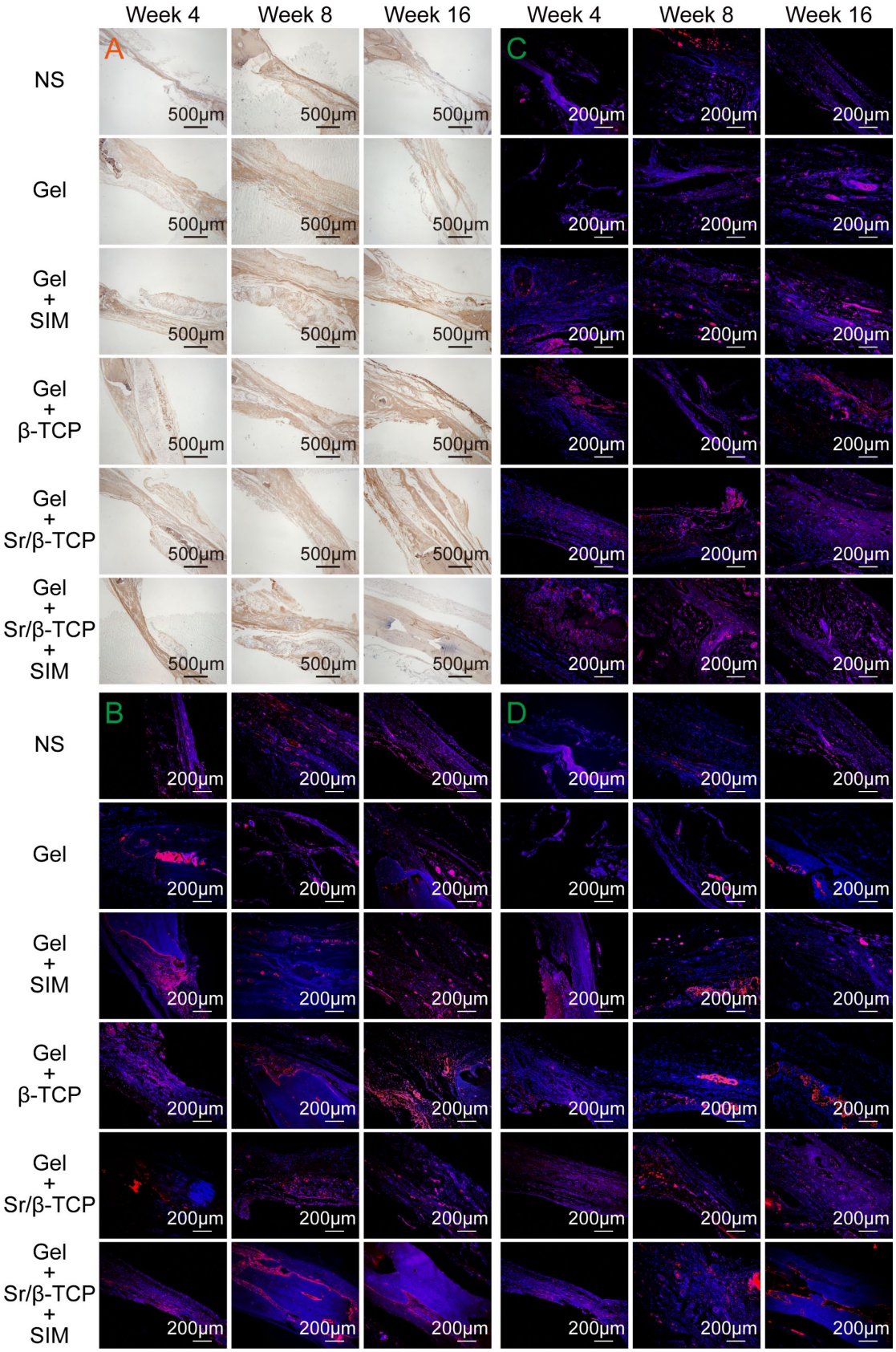

Fig. S8 Immunohistochemical and immunofluorescent analysis of bone regeneration in rat cranial defects of the indicated groups. (A) Immunohistochemical micrographs of COL-I. Immunofluorescence images of (B) OCN, (C) RUNX2, and (D) OPN.

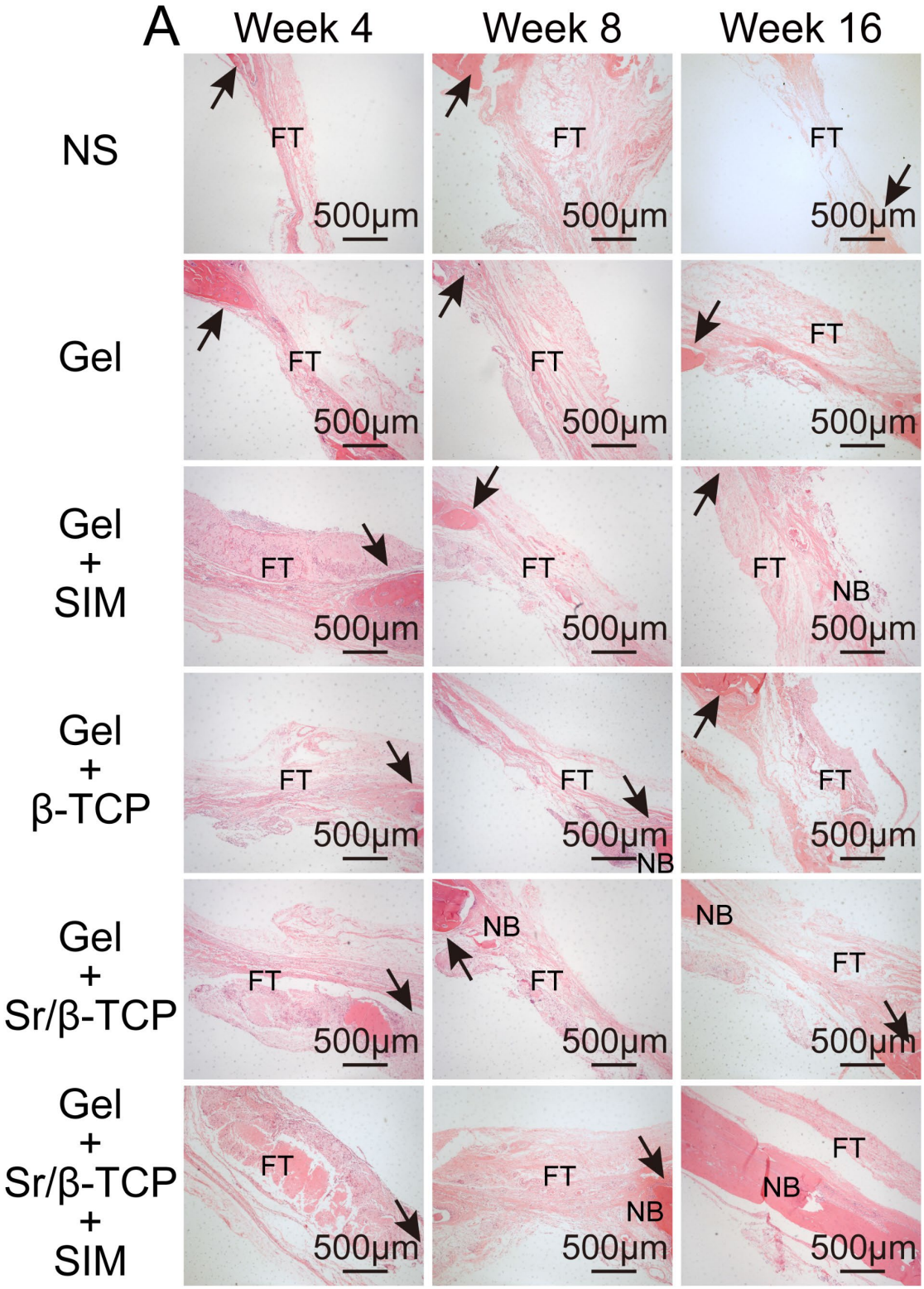

Fig. S9 Histological analysis of bone regeneration in rat cranial defects. The representative micrographs of H&E staining of cranial defect sections. (Arrows denote the boundary between new bone and host bone. NB: new bone, FT: fibrous tissue.)

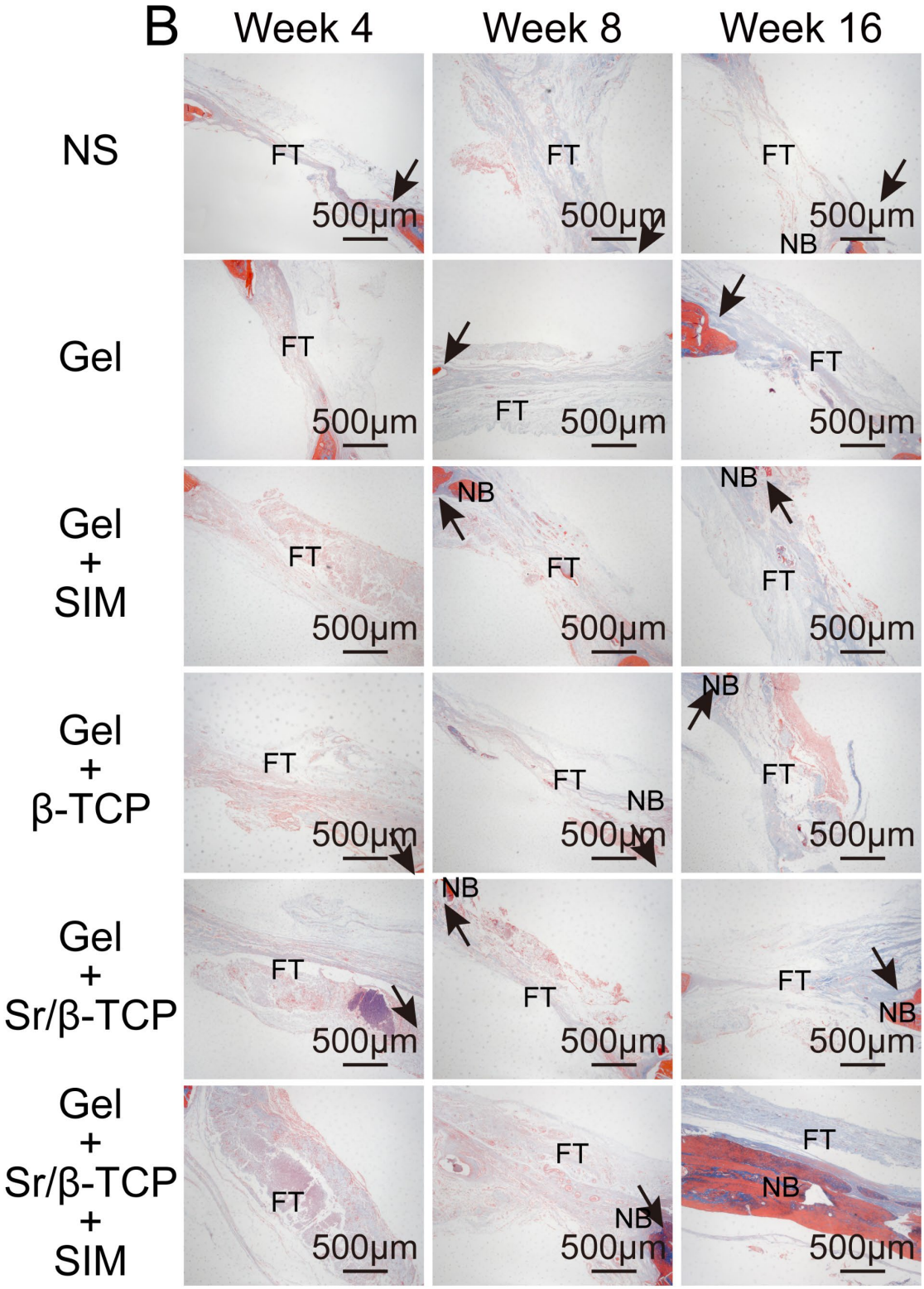

Fig. S10 Histological analysis of bone regeneration in rat cranial defects. The representative micrographs of Masson staining of cranial defect sections. (Arrows denote the boundary between new bone and host bone. NB: new bone, FT: fibrous tissue.)

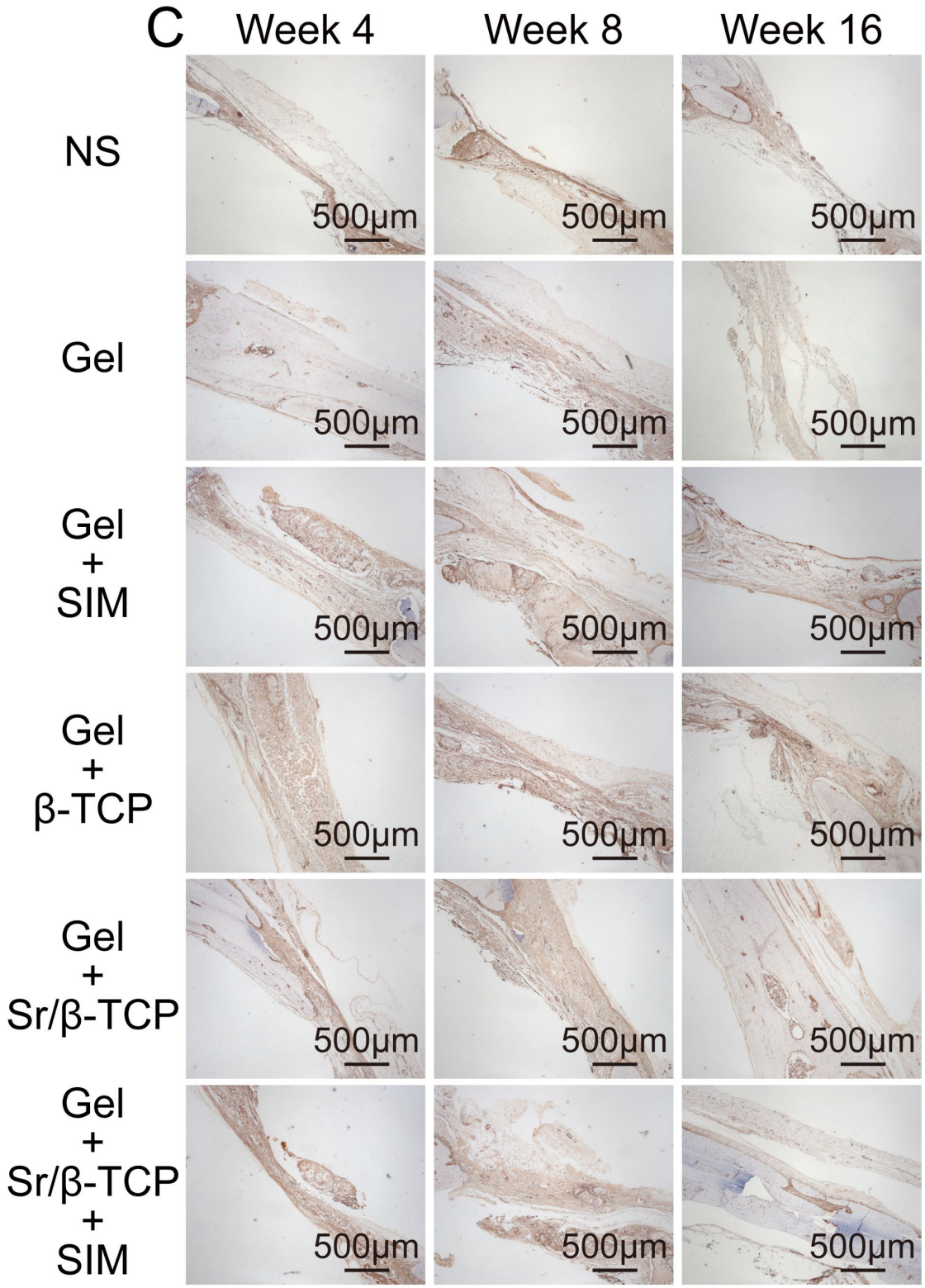

Fig. S11 Immunohistochemical analysis of bone regeneration in rat cranial defects. The representative micrographs of immunohistochemical staining for OCN of cranial defect sections.

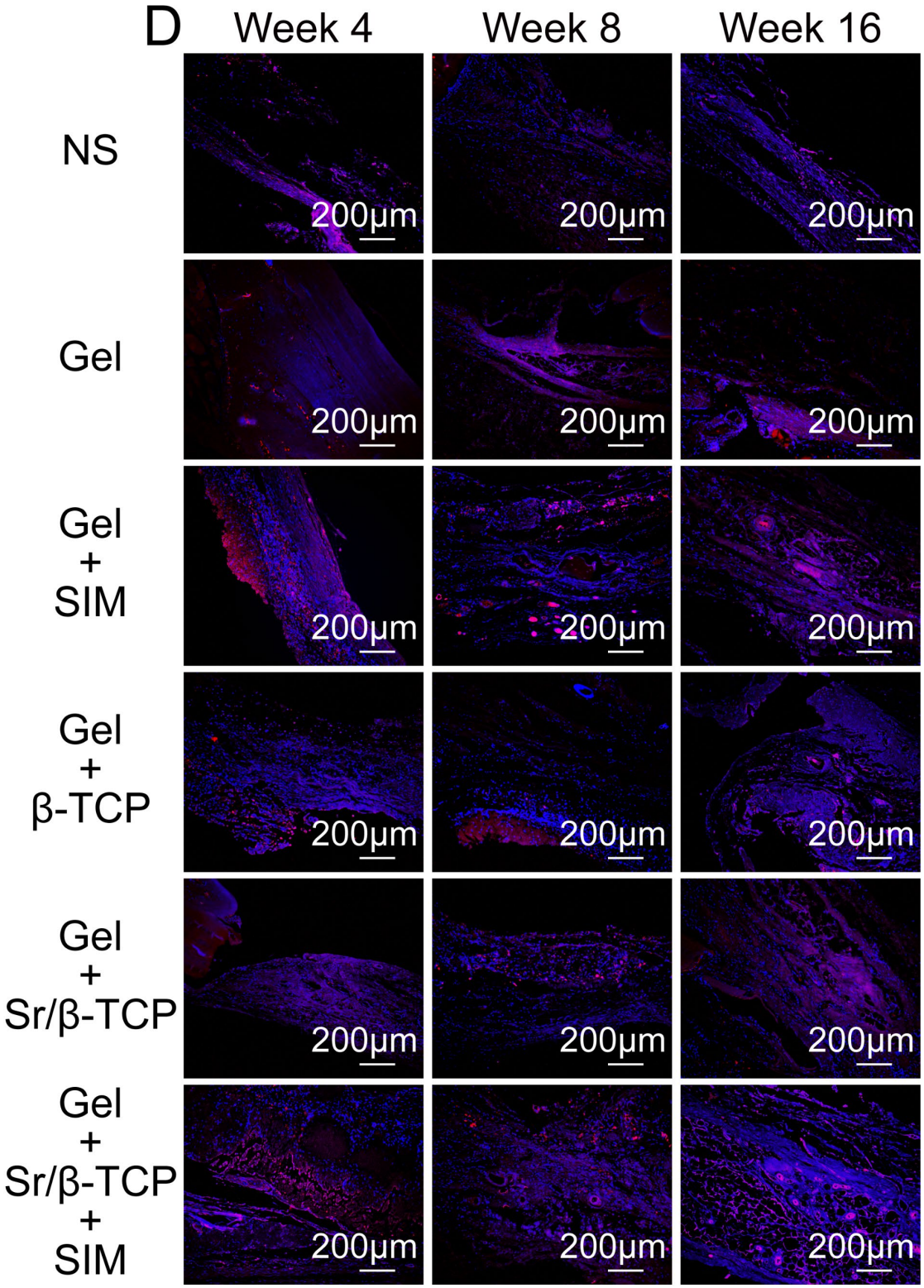

Fig. S12 Immunofluorescent analysis of bone regeneration in rat cranial defects. The representative micrographs of immunofluorescent staining for COL-I of cranial defect sections.